

Fluid Dynamic Simulation of Odour Measurement Chamber

Giacomo Viccione*, Daniele Spiniello, Tiziano Zarra, Vincenzo Naddeo

Department of Civil Engineering, University of Salerno, via Giovanni Paolo II n. 132, 84084 Fisciano (SA), Italy
 (*e-mail: gviccion@unisa.it ; Tel. +39 089 963408; Fax +39 089 968806)

Arrays of chemical sensors, generally used in electronic noses (e.noses), yield a unique pattern for a given mixture of odours. In recent years, there has been an increasing interest in applications of e.noses for the characterization and monitoring of environmental odours. While they have been around over the last three decades, little effort has been devoted to the development of the measurement chamber. Within it, all sensors are placed in contact of the flux of air to characterize in terms of odours. A measurement chamber must ensure standardized conditions in term of temperature, humidity and contact time of inflow air with the sensor surfaces.

Aim of this work is to numerically analyse the fluid dynamic performance of measurement chambers with different geometry in order to improve sensor response signals in terms of stability, reproducibility and response time. The Fluid dynamic study was carried out by a Computational Fluid Dynamic (CFD) commercial software.

Results show an objective methodological approach that can be used to design measurement chamber for electronic noses.

1. Introduction

Odour emissions from industrial plants (e.g. manufacturing plants, wastewater treatment plants, etc.) into the atmosphere may cause significant public concerns and complaints (Ampuero et al., 2003, Zarra et al., 2008, Lehtinen et al., 2012). Effects of offensive smells should be assessed as well as proper actions must be taken for the control of odour annoyance according to related local legislations, when existing. One of the limits in the diffusion of legislation is the difficult in the standardization of the measurement of odour exposure in ambient air.

Odours exposure can be continuously monitored by multisensory array systems commonly known as electronic noses (e.noses) (Gardner et al., 1994, Belgiorno et al., 2013, Capelli et al., 2014). E.noses are generally composed by a sampling system, a measurement chamber, a multi-sensor array, a data acquisition system and a pattern recognition algorithm (Pioggia et al., 2007).

Up to date, many researches have studied the performance of different combination of sensors in odours detection and relative pattern recognition (Zarra et al., 2009, Giuliani et al., 2012), on other way little effort seems to have been made to study the optimization of the measurement chamber in terms of proper definition of chamber size and shape (Di Francesco et al., 2005), spatial displacement of sensors (Lezzi et al., 2001), allocation and geometry of a diffuser (Falcitelli et al., 2002, Pan et al., 2009).

In order to guarantee proper sensors response, it is essential to ensure gas sample concentration at the sensors as uniform and steady as possible. In addition, time exposure, needed to record an "odour signature" and related to the modulation frequency, must be long enough to appropriately capture volatilized chemical compounds.

The work here presented, based on a previous numerical study (Viccione et al., 2012), aims to further clarify the fluid dynamic behaviour of a sensor chamber in order to guarantee homogeneous flow conditions, that is a volatile sample moving under nearly steady conditions and to minimize the presence of regions occupied by the pre-existing air as well as by stagnant and/or recirculating volatile vortices. Volatile sample motion is solved in space and time by integrating Navier–Stokes equations, written for compressible fluids. The k-eps turbulence model is added for problem closure. Refer to our previous work (Viccione et al., 2012) about the way ruling equations are solved in time over the computational domain.

2. Materials and methods

2.1 Measurement chamber

The measurement chamber, designed and patented by the SEED division of the University of Salerno (Italy), was simulated according to the previous study of Viccione et al., 2012. The present study is aimed at focusing in more detail the fluid dynamic behaviour inside the chamber. The e.Nose system called seedOA (Simple Environmental Electronic Device for Odour Application) consists of a measurement chamber equipped by sensors polarly distributed over two horizontal layer: 2 specific gas sensors (NH_3 and H_2S), 12 metal oxides non-specific gas sensors and 2 internal conditions control sensors (humidity and temperature). They were selected on the basis of the potentially odorous substances emitted from the investigated type of plant according to previous studies (Zarra et. al, 2012). In the following, sensors belonging to the lower and upper horizontal layers will be denoted by $S_{j|j=1,\dots,8}$ and $S_{j|j=9,\dots,16}$ respectively. A diffuser of height $h_d=0.06\text{m}$, comprehending inner channels connected to the inlet, is placed in the lower-central part of the chamber with the aim of spreading the volatile sample nearby the sensors, hitting them in a way that surface exposure is as higher as possible. The apparatus is modelled in a Computer Aided Design (CAD) environment. Each sensor is built by merging a cylinder (radius $r_s=0.015\text{m}$; height $h_s=0.017\text{m}$) with a hemisphere (reactive part). Refer to our previous work (Viccione et al., 2012) for a detailed description of the diffusers adopted (Figure 1) as well as the way the computational domain is spatially discretized.

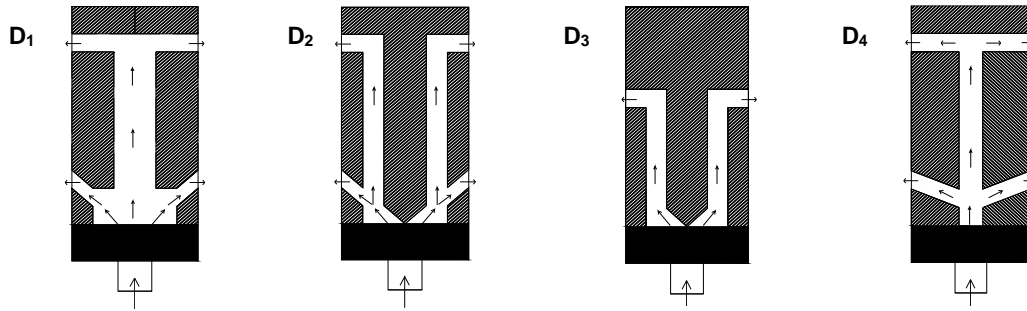


Figure 1. Vertical cross sections of the four diffusers ($D_1 - D_4$) employed in the present investigation.

2.2 Procedure for retrieving the average volume fraction of the inflow gas sample (IGS) nearby sensors

In this work, fluid dynamic variables are numerically computed and analyzed by varying the volatile discharge conveyed in, from $Q_0=10^{-6}\text{m}^3/\text{s}$ (60ml/min) to $Q_{10}=10^{-5}\text{m}^3/\text{s}$ (600ml/min). In the following, the generic discharge is defined as Q_m , $m \in [1, 10]$.

The computational domain is discretized into cubic cells, the size of each one is $2 \cdot 10^{-3}\text{m}$ (2mm). The subclass of cells in the proximity of the reactive sensor's surface is then defined by intersecting sensors with the mesh grid. From such collection, the average volume fraction of the inflow gas sample (IGS) $\langle VV_{v,S_j,D_k} \rangle(t)$ as function of time, at the specific sensor $S_{j|j=1,\dots,16}$, for the specific diffuser $D_{k|k=1,\dots,4}$, is finally computed, extracting the information stored inside each neighbouring cell. A further spatial averaging is then made for all the 16 sensors, yielding the aggregated variable $\langle VV_{v,S_1-S_{16},D_k} \rangle(t)$.

2.3 Procedure for the identification of non-effective regions

As volatile sample is conveyed inside the measurement chamber through the diffuser, pre-existing air is expelled from the outlet placed in the upper-central side of the apparatus. Despite the injected gas takes over the available space inside the chamber over time, yet a portion of it remains trapped.

The volume fraction $VV_{\text{res},D_k}(t)$ related to such non-effective regions (subscript "res" stands for volume residual) as function of time t , diffuser employed $D_{k|k=1,\dots,4}$, and discharge Q_m , conveyed in, is then derived.

2.4 Procedure for retrieving the average contact time at the sensors

A roughly estimate of the average contact time at the sensors as function of the discharge Q_m conveyed inside the chamber is here proposed. Detection time DT_{c,D_k} at the "chamber scale" is first computed as follows:

$$DT_{c,D_k}(t) = (1 - VV_{\text{res}}) \frac{V_C}{Q_m} \quad (1)$$

where $V_c = 4.45 \cdot 10^{-4} \text{m}^3$ is the inner volume available. The term between parentheses represents the volume percent taken by volatile sample, effectively moving toward the outlet. The average contact time at the sensors $\langle CT_{S1-S16, Dk} \rangle$ is then derived by scaling $DT_{c, Dk}$ of h_s/h_c , being $h_c=0.07\text{m}$ the height of the inner region of the chamber:

$$\langle CT_{S1-S16, Dk}(t) \rangle = \frac{h_s}{h_c} DT_{c, Dk}(t) \quad (2)$$

3. Results

3.1 Volume fraction trends of IGS nearby sensors

Sensors' response is reliable whether volatile concentration nearby reactive surfaces is not affected by significant temporal fluctuations. In addition, the higher is the corresponding value, the greater is the fraction of volatile sample sniffed by sensors. In Figure 2, the average volume fraction of IGS $\langle VV_{v, S_j, D_k} \rangle(t)$ as function of time, is given for each sensor $S_{j|j=1, \dots, 16}$ and diffuser $D_{k|k=1, \dots, 4}$, for the reference volatile discharge $Q_5=5 \times 10^{-6} \text{m}^3/\text{s}$.

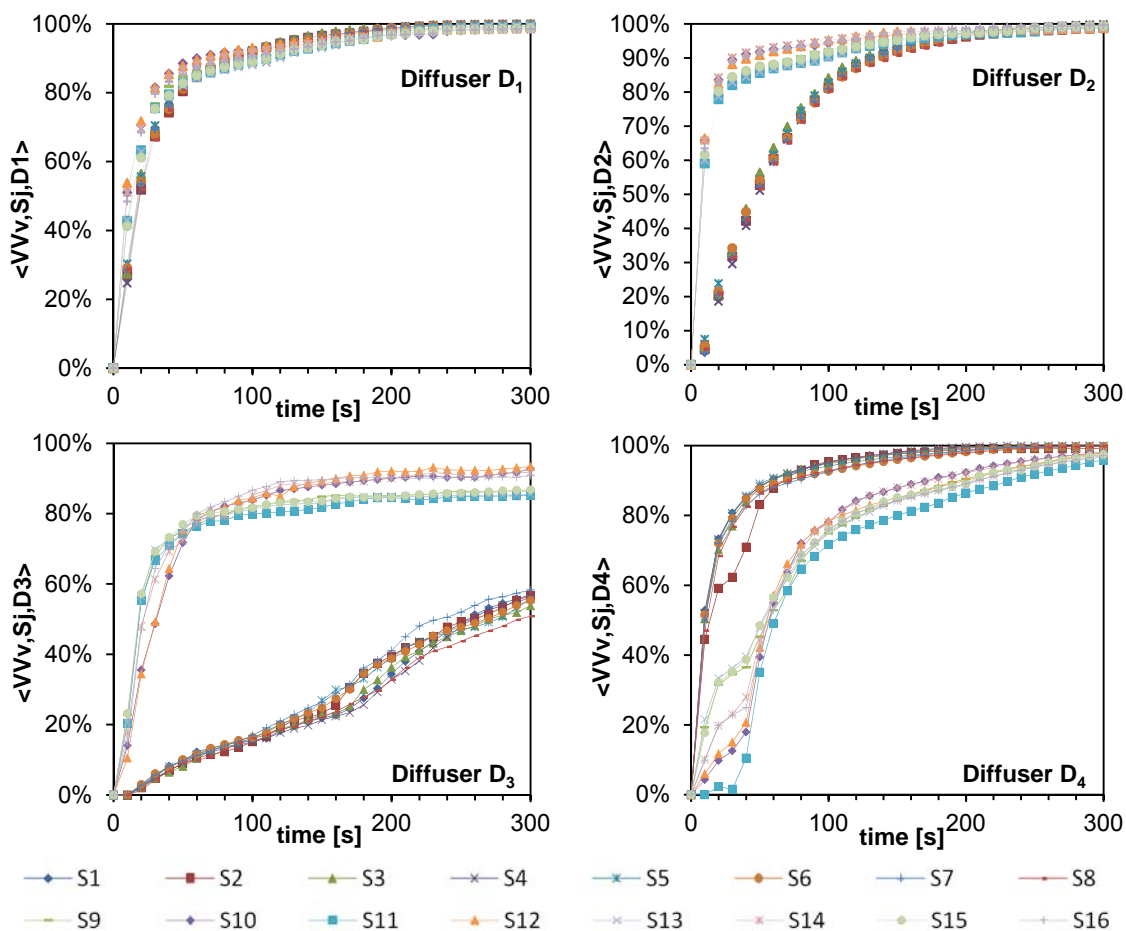


Figure 2. Average volume fraction of IGS $\langle VV_{v, S_j, D_k} \rangle(t)$ at each sensor and for each diffuser employed, for volatile discharge $Q_5=5 \times 10^{-6} \text{m}^3/\text{s}$.

As general behaviour, there is an abrupt increase of the average volatile fraction at the sensors within the first minute (60s) of injection. This is basically due to the fact that the volatile sample is channelized and expelled toward the measurement devices. Exceptions occurred for sensors placed in the lower horizontal layer, in the case of chambers with diffuser D₂, D₃ and D₄. For the former and the latter ones, this is essentially due to a not optimal design of size and inclination of diffuser's lower pipes. With respect to diffuser D₃ the situation is even worse for the lack of them. Inner pipes should be therefore properly designed and foreseen upon each sensor. Still, diffuser D₃ represents the only case for which the average volatile fraction does not reach the maximum value of 100% after 5 minutes of simulating process.

Volatile concentrations are expected to growth in time by increasing the flowing gas injected inside the chamber. In the following Figure 3 spatial averaged volatile fraction $\langle VV_{v,S1-S16,Dk} \rangle(t)$ is shown for the minimum, reference and maximum discharge Q_1 , Q_5 and Q_{10} , just for the sake of clarity. As can be noted from the upper side of Figure 3 lower discharges (compared to the reference $Q_5=10^{-5} \text{ m}^3/\text{s}$) do not allow sniffing “pure” volatile sample by sensors, as the average field $\langle VV_{v,S1-S16,Dk} \rangle$, for each k , is always lower than 100%. Interestingly enough, trends for diffuser D_1 (solid red lines) seems to reach an asymptotic behaviour above Q_5 (compare trends depicted in the central and lower side of Figure 3). This is due to the reaching of a system geometry spatial invariance respect to a discharge threshold value (lower limit). Diffuser D_3 (dashed brown lines in Figure 3) exhibits the worst behaviour. The averaged volatile fraction $\langle VV_{v,S1-S16,Dk} \rangle(t)$ reaches the maximum value only for the maximum discharge Q_{10} injected in.

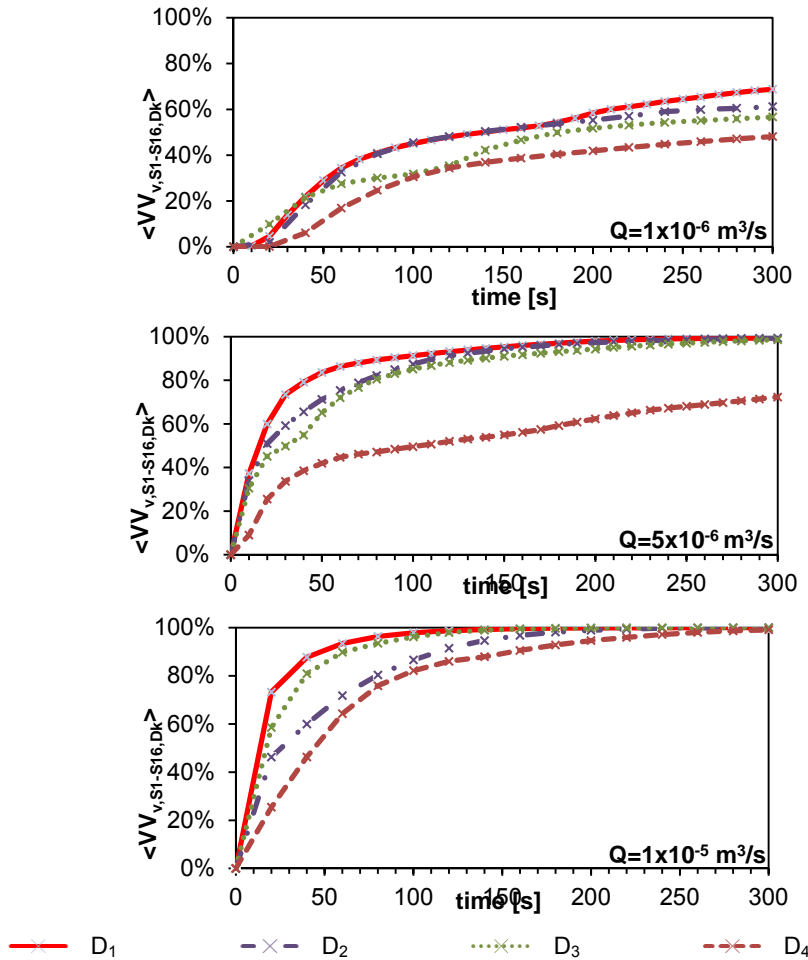


Figure 3. Spatial averaged volatile concentration $\langle VV_{v,S1-S16,Dk} \rangle(t)$ for all sensors and for each diffuser employed, for volatile discharge $Q_1=10^{-6} \text{ m}^3/\text{s}$, $Q_5=5 \times 10^{-6} \text{ m}^3/\text{s}$, $Q_{10}=10^{-5} \text{ m}^3/\text{s}$.

3.2 Identification of non-effective regions

Pre-existing air, stagnant or recirculating regions inside the chamber need to be minimized. Reasons are twofold: on one hand, sensors reactive surfaces should be in contact with the volatile sample, once nearly steady conditions are established (Viccione et al., 2012); on the other hand, effective-non effective air mixing should be limited, otherwise sensors readings may be distorted. The latter aspect is relevant, as turbulent motion takes place for the cases here investigated. In Table 1, volume fractions $VV_{res,Dk}$ related to non-effective regions, as function of diffuser employed $D_{k|k=1,\dots,4}$, and discharge Q_m , are given at 5min of simulation process. Non effective regions cannot be nullified. As can be seen from Table 1, there is a lower asymptotic limit of (e.g., about 12% for Diffuser D2) of the available inner space. Such a value is essentially due to the air entrapped inside peripheral regions next to the inner chamber surface. In addition, nearly steady state is reached only above certain volatile discharges, depending on the diffuser adopted, as summarized in the following Table 2.

Table 1: Volume fractions $VV_{res,Dk}(t)$ at 5min (300sec) of simulation process. See next Table 2 for corresponding cases for which nearly steady state is reached.

Diffuser	Q ₁	Q ₂	Q ₃	Q ₄	Q ₅	Q ₆	Q ₇	Q ₈	Q ₉	Q ₁₀
D ₁	45%	39%	22%	19%	18%	17%	16%	15%	14%	14%
D ₂	58%	38%	22%	19%	17%	16%	14%	13%	12%	12%
D ₃	59%	49%	45%	40%	31%	28%	21%	18%	16%	15%
D ₄	52%	30%	24%	19%	18%	18%	17%	17%	17%	16%

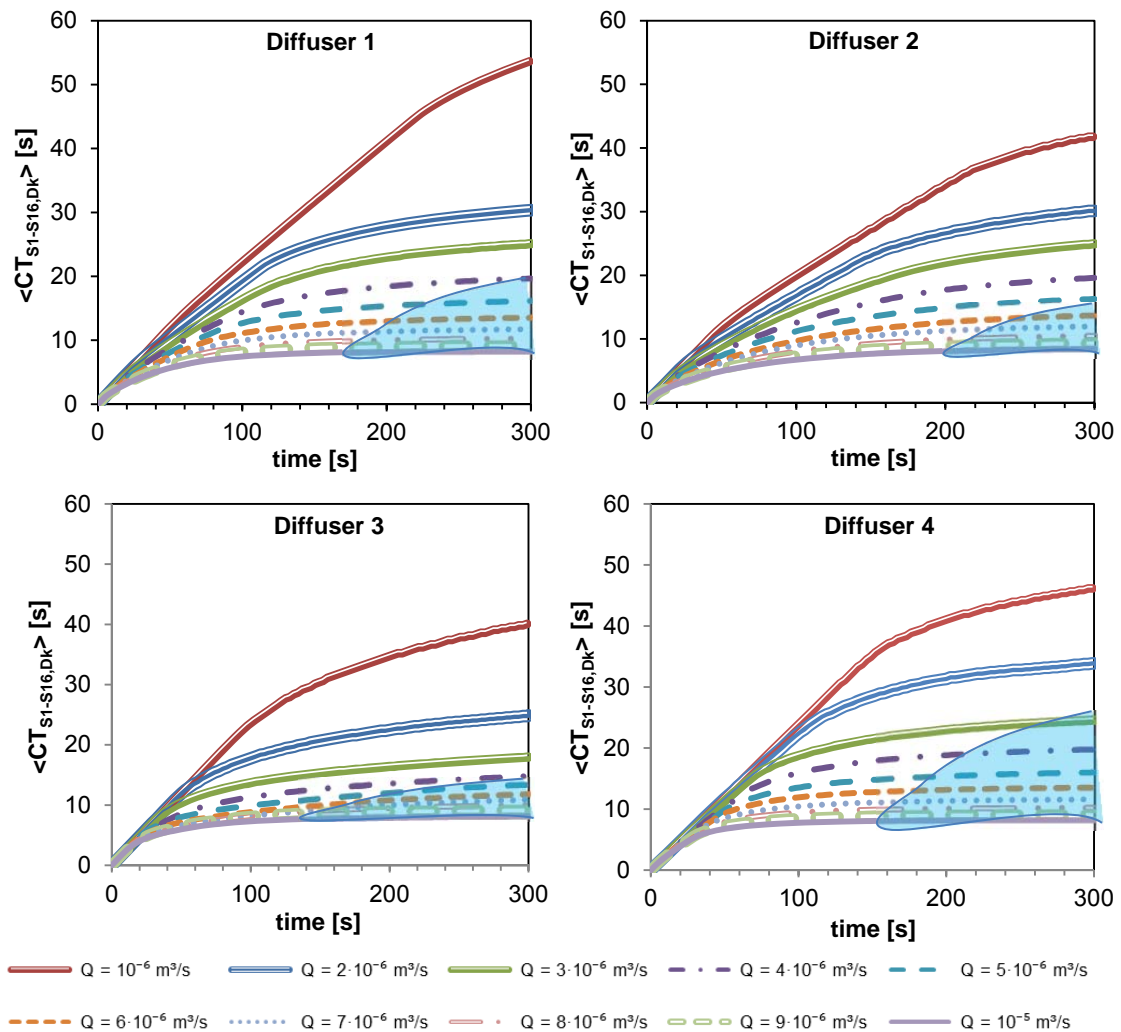


Figure 4. Average contact time at the sensors $\langle CT_{S_1-S_{16}, D_k} \rangle$. Shadow cyan coloured areas indicate when the field is stable.

3.3 Average contact time at the sensors

Sensors time exposure, needed to record a reliable odour signature, must be long enough to appropriately capture volatilized chemical compounds. In Figure 4, the contact time $\langle CT_{S_1-S_{16}, D_k} \rangle$ roughly estimated as specified in Section 2.3, is given as function of time t , diffuser employed $D_k |_{k=1, \dots, 4}$, and discharge Q_m . As can be noted, average contact times $\langle CT_{S_1-S_{16}, D_k} \rangle$ increase as volatile discharges Q_m decrease.

Table 2: Periods (in seconds) needed for the achievement of the nearly steady condition (left) and Stable Contact Times (SCT, in seconds - right) for each diffuser and discharge, within 5min of simulation process. (N.R. stands for "not reached")

Diffuser	Q ₁	Q ₂	Q ₃	Q ₄	Q ₅	Q ₆	Q ₇	Q ₈	Q ₉	Q ₁₀
D ₁	N.R. N.R.	N.R. N.R.	N.R. N.R.	N.R. 19.9	290 16.2	286 13.3	280 11.5	274 10.2	268 9.5	261 8.8
D ₂	N.R. N.R.	N.R. N.R.	N.R. N.R.	N.R. N.R.	N.R. 16.1	297 14.3	293 11.8	288 10.3	283 9.6	277 9.1
D ₃	N.R. N.R.	N.R. N.R.	N.R. N.R.	N.R. N.R.	N.R. 13.8	N.R. 12.4	N.R. 11.9	295 11.0	290 9.4	288 8.2
D ₄	N.R. N.R.	N.R. N.R.	N.R. 23.8	N.R. 19.9	288 14.5	275 13.2	259 11.6	241 10.2	220 9.6	198 8.8

Horizontal asymptotes (right side for each subplot, within the shadow cyan coloured area) appear for certain conditions as specified in Table 2. They indicate that Stable Contact Times (SCT) are attained within 5 min of simulating process.

4. Conclusions

Fluid dynamic computation of measurement chamber used in a new type of eNose was investigated. In this study, the effects of diffuser employed and volatile discharge were examined as function of both geometry and injected flow rate. The average volume fraction of the inflow gas sample (IGS) nearby sensors, the amount of non-effective regions intended as stagnant, recirculating zones, as well as by the pre-existing air, the average contact time at the sensors were derived and discussed.

This study was performed by creating a 3D model of the sensor chamber, discretizing the computational domain in finite volumes and numerically solving the transport equations of both momentum and mass (Navier-Stokes equations). Four types of geometries of diffuser have been simulated.

Numerical simulations showed the key role of the geometry of diffuser in the chamber in order to minimizing the time for the achievement of the nearly steady conditions and ensure a sufficient contact time at the sensors.

References

- Ampuero, S., Bosset, J.O., 2003. The electronic nose applied to dairy products: A review, *Sensors and Actuators, B: Chemical*, 94 (1), 1-12.
- Belgiorno V., Naddeo V., Zarra T., 2013. *Odour Impact Assessment Handbook*. John Wiley & Sons, Inc., New York, ISBN: 978-1-119-96928-0
- Capelli, L., Dentoni, L., Sironi, S., Del Rosso, R., 2014, The need for electronic noses for environmental odour exposure assessment, *Water Science and Technology*, 69 (1), 135-141.
- Di Francesco F., Falcitelli M., Marano L., Pioggia G., 2005. A radially symmetric measurement chamber for electronic noses, *Sensors and Actuators, B: Chemical*, 105(2), 295–303.
- Falcitelli M., Benassi A., Di Francesco F., Domenici C., Marano L., Pioggia G., 2002. Fluid dynamic simulation of a measurement chamber for electronic noses, *Sensors and Actuators B: Chemical*, 85(1–2), 166-174.
- Gardner J.W., Bartlett P.N., 1994. A brief history of electronic noses. *Sensors and Actuators, B: Chemical*, 18–19, pp. 211–220.
- Giuliani, S., Zarra, T., Nicolas, J., Naddeo, V., Belgiorno, V., Romain, A.C., 2012. An alternative approach of the e-nose training phase in odour impact assessment, *Chemical Engineering Transactions*, 30, 139-144.
- Lehtinen, J., Giuliani, S., Zarra, T., Reiser, M., Naddeo, V., Kranert, M., Belgiorno, V., Romain, A.C., Nicolas, J., Sówka, I., Wang, K.Y., Kalogerakis, N., Lazaridis, M., 2012. Case Studies for Assessment, Control and Prediction of Odour Impact, *Odour Impact Assessment Handbook*, 205-283.
- Lezzi A.M., Beretta G.P., Comini E., Faglia G., Galli G., Sberveglieri G., 2001. Influence of gaseous species transport on the response of solid state gas sensors within enclosures, *Sensors and Actuators, B: Chemical*, 78, 144–150.
- Pan L., Yang S. X., 2009. An Electronic Nose Network System for Online Monitoring of Livestock Farm Odors, *IEEE/ASME Transactions on Mechatronics*, 14(3), 371-376.
- Pioggia G., Ferro M., Di Francesco F., 2007. Towards a Real-Time Transduction and Classification of Chemoresistive Sensor Array Signals, *IEEE sensors journal*, 7(2), 237-244.
- Viccione G., Zarra T., Giuliani S., Naddeo V., Belgiorno V., 2012. Performance study of e-nose measurement chamber for environmental odour monitoring, *Chemical Engineering Transactions*, 30, 109-114, DOI: 10.3303/CET1230019.
- Zarra, T., Naddeo, V., Belgiorno, V., Reiser, M., Kranert, M., 2008. Odour monitoring of small wastewater treatment plant located in sensitive environment, *Water Science and Technology*, 58 (1), 89-94.
- Zarra, T., Naddeo, V., Belgiorno, V., Reiser, M., Kranert, M., 2009. Instrumental characterization of odour: A combination of olfactory and analytical methods. *Water Science and Technology*, 59 (8), 1603-1609.
- Zarra, T., Giuliani, S., Naddeo, V., Belgiorno, V., 2012. Control of odour emission in wastewater treatment plants by direct and undirected measurement of odour emission capacity. *Water Science and Technology*, 66 (8), 1627-1633.